On the Integral Equation Derived from the Linearized BGK Equation for the Steady Couette Flow

Shidong Jiang
Department of Mathematics Sciences, New Jersey Institute of Technology, Newark, New Jersey 07102, USA
Li-Shi Luo
Department of Mathematics and Statistics, Old Dominion University, Norfolk, VA 23529, USA
Beijing Computational Science Research Center, Beijing 10084, China

Abstract

The integral equation for flow velocity $u(x, k)$ derived from the linearized Bhatnagar-Gross-Krook kinetic equation for the steady Couette flow is studied in detail both theoretically and numerically in a wide range of the Knudsen number k. First, it is shown that the integral equation is a Fredholm equation of the second kind in which the norm of the compact integral operator is less than 1 on L^p for any $1 \leq p \leq \infty$ and thus there exists a unique solution to the integral equation *via* the Neumann series. Second, it is shown that the solution is logarithmically singular at the end points. More precisely, if $x = 0$ is an end point, then the solution can be expanded as a double power series of the form $\sum_{n=0}^{\infty} \sum_{m=0}^{\infty} c_{n,m} x^n (x \ln x)^m$ on a small interval $x \in (0, a)$ for some $a > 0$. And third, a high-order adaptive numerical algorithm is designed to compute the solution numerically to high precision. The solutions for the flow velocity $u(x, k)$, the stress $P_{xy}(k)$, and the half-channel total mass flow rate $Q(k)$ are obtained in a wide range of the Knudsen number $0.003 \leq k \leq 10.0$; and these solutions are accurate for at least twelve significant digits or better, thus they can be used as benchmark solutions.

1 Introduction

In small scale devices, such as microfluidics, gaseous flows may become highly nonequilibrium, thus it is required to solve the Boltzmann equation or other kinetic equations (cf. reviews [18, 35], monographs [21, 7, 9, 8, 20, 33], and relevant references therein). Kinetic equations evolve in phase space $(\boldsymbol{x}, \boldsymbol{\xi})$, where $\boldsymbol{\xi} := \dot{\boldsymbol{x}}$ is the particle velocity, thus numerical solutions of kinetic

equations are far more challenging and demanding than numerical solutions of hydrodynamic equations in physical space $\boldsymbol{x}$. To mitigate the difficulty, one often considers the linearized Boltzmann equation or simpler model kinetic equations, such as the Bhatnagar-Gross-Krook (BGK) equation [4].

There are several canonical flows which have been studied for long time, including Kramer's flow, Poiseuille flow, and Couette flow; and there has been a systematic and persistent effort to obtain accurate numerical solutions of the kinetic equations corresponding to these flows [17, 36, 2, 11, 12, 24, 25, 13, 26, 34, 31, 3, 10, 27, 30, 15, 40]. Accurate solutions of these canonical flows have been used as benchmark data to test numerical schemes [31, 3, 10, 27, 40].

For the aforementioned canonical flows, the linearized BGK equation with Maxwell diffusive boundary conditions leads to Fredholm integral equations of the second kind with singular kernels, and there have been continuous effort to obtain accurate numerical solutions of the integral solutions for the canonical flows [31, 3, 10, 27, 40, 38, 37]. However, it appears that some advanced modern techniques developed in the last few decades for solving integral equations with singular kernels, the inhomogeneous term and solutions have yet to be fully utilized in the community of rarefied gas dynamics (RGD). Indeed, accurately solving these integral equations requires high order quadratures for evaluating the involved (weakly) singular integrals and a proper discretization scheme to capture the singularities of the solution and the inhomogeneous term at the end points. However, currently popular methods for solving these integral equations use the Meijer G-function to compute the singular kernels [27, 40], apply smooth Gaussian quadrature to evaluate the singular integrals, and represent the solution with some global expansion of smooth functions or piecewise polynomials on equispaced subintervals. Obviously, the use of Meijer G-function for the evaluation of the singular kernel function (*e.g.*, the Abramowitz function in many cases) is very likely to suffer from catastrophic cancellation for large values of the argument, as observed previously [39]. The application of smooth Gaussian quadrature to evaluate the singular integrals either results in a very low accuracy or demands an excessively large number of nodes required for the quadrature. Finally, the representation of the solution by using globally smooth polynomial expansion or piecewise polynomials on equispaced subintervals cannot capture the singularities of the solution and the inhomogeneous function. Thus, the predominant methodologies currently employed in the RGD community fail to obtain high-precision benchmark solutions of

these integral equations [39]. This is especially true in the case of obtaining high-precision benchmark solutions of the linearized BGK equation for canonical flows [31, 3, 10, 27, 40]. For example, Loyalka and Tompson [27] use the Nyström method with Gauss-Kronrod quadrature to solve the integral equation for Kramers' problem, they were only able to obtain the flow velocity with an accuracy of about 7 digits even though the largest quadrature order is 1,312 and a precision of 60 digits is required for the arithmetic computation More recently, [40] use the same technique with Gauss-Legendre quadrature to study steady and oscillating Couette flows, and with a large linear system of size $12,800^2 = 163,840,000$ and a precision of 30 digits, they are only able to obtain the velocity between 5 and 8 significant digits for he Knudsen number k between 0.01 and 100.0. While these results [27, 40] may be the most accurate to date, they do not even attain the accuracy of double-precision while they also demand significant computational effort.

In this paper, we study the following integral equation which is derived from the linearized BGK equation for the steady Couette flow [21, 7, 9, 8, 20, 33]:

$$u(x,\, k) - \frac{1}{k\sqrt{\pi}} \int_{-1/2}^{1/2} J_{-1}\left(\frac{|x-y|}{k}\right) u(y)\mathrm{d}y = f(x,\, k), \tag{1a}$$

$$f(x,\, k) := \frac{1}{2\sqrt{\pi}} \left[J_0\left(\frac{1/2-x}{k}\right) - J_0\left(\frac{1/2+x}{k}\right)\right], \tag{1b}$$

where k is the Knudsen number and J_n is the n-th order Abramowitz function defined by

$$J_n(x) = \int_0^\infty t^n e^{-t^2 - x/t}\mathrm{d}t. \tag{2}$$

It is easy to show that the kernel function J_{-1} has both absolute and logarithmic singularities on the diagonal, and that the right hand side function is logarithmically singular at both end points. We will first study in detail the singularities of the solution of (1a) at the end points. When the left end point is shifted to the origin, the solution of (1a) contains singular terms $(x \ln x)^n$ for $n = 1, 2, \ldots$. We would like to point out that while the leading order singularity $x \ln x$ in the solution $u(x,\, k)$ of (1a) has been observed previously [18, 32], higher-order singular terms (*i.e.*, $(x \ln x)^n$ for $n > 1$) do not seem to have been revealed in the literature. We then apply a high-order adaptive collocation method to solve (1a) numerically. Our numerical method has the

following features. First, in order to capture the singularities of the solution and the right hand side function, the collocation points are chosen adaptively with finer and finer grids toward the end points. Second, in order to evaluate the involved integrals accurately, a high-order generalized Gaussian quadrature is applied to compute (weakly) singular integrals and an automatic adaptive Gaussian quadrature is used to compute (nearly) singular or smooth integrals to high precision (10^{-30}). This way, we are able to provide 12-digit benchmark solutions with a quite reasonable computational cost.

The remainder of the paper is organized as follows. Section 2 contains certain analytic properties of the Abramowitz function and lists some integral formulas involving logarithmic and power functions. Section 3 summarizes our main theoretical results, which fully reveal the mathematical properties of the solution $u(x,\, k)$. Section 4 describes the numerical method to be used to solve (1a). Section 5 presents the numerical results for the flow velocity $u(x,\, k)$, the stress $P_{xy}(k)$, and the half-channel total mass flow rate $Q(k)$ with a wide range of Knudsen number $0.003 \leq k \leq 10.0$, all of which are accurate for at least twelve significant digits. Finally, Section 6 concludes this paper.

2 Mathematical Preliminaries

In this section, we collect some known analytic properties of the Abramowitz function J_n and list some formulas for certain definite and indefinite integrals involving logarithmic and power functions, which are used in the proofs of Theorems 1, 2 and Corollary 2.

The Abramowitz function J_n satisfies the following differential and recursive relationships [1, 29]:

$$J'_{n+1}(x) = -J_n(x), \tag{3a}$$
$$2J_n(x) = (n-1)J_{n-2}(x) + xJ_{n-3}(x) \tag{3b}$$

Also, J_n can be written in the following form:

$$J_n(x) = f_n(x) + xg_n(x) + x^{n+1}h_n(x)\ln(x), \qquad n \geq -1, \tag{4}$$

where f_n, g_n, h_n are all power series of x^2 with $h_n(0) \neq 0$. The above formula and its asymptotic expansions in both small and large x are used to compute

the value of J_n [29]. In particular, we have:

$$2J_1(x) = \sum_{m=0}^{\infty} (a_m \ln x + b_m)\, x^m \tag{5}$$

with $a_0 = a_1 = 0$, $a_2 = -1$, and $b_0 = 1$, $b_1 = -\sqrt{\pi}$, $b_2 = 3(1-\gamma)/2$,

$$a_m = \frac{-2a_{m-2}}{m(m-1)(m-2)}, \quad b_m = \frac{-2b_{m-2} - (3m^2 - 6m + 2)a_m}{m(m-1)(m-2)}, \qquad m \geq 3, \tag{6}$$

where $\gamma \approx 0.5772156649015328606$ is Euler's constant.

The following properties of J_n follow from the definition of J_n (2) and (3a) and will be used in Section 3.

1. $J_n(x) > 0$ for any $x > 0$;
2. $J_n(x)$ is monotone decreasing on $[0, \infty)$;
3. $J_n(x)$ is convex on $[0, \infty)$;
4. $J_0(0) = \sqrt{\pi}/2$.

The following definite and indefinite integrals involving logarithmic and power functions will be used in the proofs of Corollary 1.

$$\int x^n (\ln x)^m \mathrm{d}x = x^{1+n} m! \sum_{i=0}^{m} \frac{(-1)^{m-i} (\ln x)^i}{(m-i)!\,(1+n)^{m+1-i}}, \qquad m,\, n \geq 0, \tag{7a}$$

$$\int x^{-1} (\ln x)^m \mathrm{d}x = \frac{1}{m+1} (\ln x)^{m+1}, \qquad m \geq 0, \tag{7b}$$

$$\int x^{-n} (\ln x)^m \mathrm{d}x = x^{1-n} m! \sum_{i=0}^{m} \frac{(\ln x)^i}{(m-i)!\,(1-n)^{m+1-i}}, \qquad m \geq 0,\, n > 1. \tag{7c}$$

$$\int_0^a (x-y)^{2k} y^n (\ln y)^m \mathrm{d}y = \sum_{i=0}^{2k} c_i x^i, \quad k,\, n,\, m \geq 0, \tag{8}$$

$$\int_0^a |x-y|(x-y)^{2k} y^n (\ln y)^m \mathrm{d}y = \sum_{i=0}^{2k+1} a_i x^i + x^{2k+n+2} \sum_{i=0}^{m} b_i (\ln x)^i, \tag{9a}$$

$$\int_0^x y^n (\ln y)^m \ln|x-y| \mathrm{d}y = \frac{x^{n+1}(\ln x)^{m+1}}{(n+1)} + x^{n+1} \sum_{i=1}^{m} \alpha_i (\ln x)^i, \tag{9b}$$

$$\int_x^a y^n (\ln y)^m \ln|x-y| \mathrm{d}y = -\frac{m\, x^{n+1}(\ln x)^{m+1}}{(n+1)(m+1)} + x^{n+1} \sum_{i=0}^{m} \beta_i (\ln x)^i + \sum_{j=0}^{\infty} \zeta_j x^j, \tag{9c}$$

$$\int_0^a y^n (\ln y)^m \ln|x-y| \mathrm{d}y = \frac{x^{n+1}(\ln x)^{m+1}}{(n+1)(m+1)} + x^{n+1} \sum_{i=0}^{m} \gamma_i (\ln x)^i + \sum_{j=0}^{\infty} \zeta_j x^j, \tag{9d}$$

where $0 < x < a - \epsilon < a \leq 1$, k, m, $n \geq 0$; and a_i, b_i, c_i, α_i, β_i, $\gamma_i (= \alpha_i + \beta_i)$ and ζ_j are all constant coefficients.

Identities (7) – (9). Identity (7a) can be found in p. 234 of [16] and identity (7b) follows by simple change of variable. Identity (7c) is obtained by applying the following integration by parts formula m times

$$\int x^{-k} (\ln x)^m \mathrm{d}x = -\frac{x^{1-k}(\ln x)^m}{(k-1)} + \frac{m}{(k-1)} \int x^{-k} (\ln x)^{m-1} \mathrm{d}x. \tag{10}$$

To prove (8), we expand

$$(x-y)^{2k} = \sum_{j=0}^{2k} C_{2k}^j x^j (-1)^{2k-j} y^{2k-j},$$

pull out x^j from the integration, and note that the following integral is finite:

$$\int_0^a y^{2k-j+n} (\ln y)^m \mathrm{d}y.$$

To prove (9a), we expand the integral as follows:

$$\begin{aligned}
&\int_0^a |x-y|(x-y)^{2k} y^n (\ln y)^m \mathrm{d}y \\
=&\int_0^x (x-y)^{2k+1} y^n (\ln y)^m \mathrm{d}y - \int_x^a (x-y)^{2k+1} y^n (\ln y)^m \mathrm{d}y \\
=&\sum_{j=0}^{2k+1} C_{2k+1}^j x^j (-1)^{2k+1-j} \left(\int_0^x - \int_x^a \right) y^{2k+1-j+n} (\ln y)^m \mathrm{d}y.
\end{aligned} \tag{11}$$

Using (7a), we have

$$\left(\int_0^x - \int_x^a \right) y^{2k+1-j+n} (\ln y)^m \mathrm{d}y = 2x^{2k+1-j+n+1} \sum_{i=0}^{m} c_i (\ln x)^{m-i} - A, \tag{12}$$

where A is a constant. Substituting (12) into (11), leads to (9a).

To prove (9b), we write $\ln(x-y) = \ln x + \ln(1-y/x)$ and make change of variable $z = y/x$, then

$$\begin{aligned}
&\int_0^x y^n (\ln y)^m \ln|x-y| \mathrm{d}y = \int_0^1 [\ln x + \ln(1-z)]\, x^{n+1} z^n (\ln x + \ln z)^m \mathrm{d}z \\
=&x^{n+1} \left[\sum_{j=0}^{m} C_m^j (\ln x)^{j+1} \int_0^1 z^n (\ln z)^{m-j} \mathrm{d}z \right. \\
&\left. + \sum_{j=0}^{m} C_m^j (\ln x)^j \int_0^1 z^n (\ln z)^{m-j} \ln(1-z) \mathrm{d}z \right],
\end{aligned} \tag{13}$$

thus (9b) follows, since each definite integral on the right side of (13) is finite.

To prove (9c), denote the integral on the left hand side of (9c) by $I_{n,m}$, then the following recurrence relationship can be easily shown by integration by parts:

$$(1+n) I_{n,m} = (a \ln a)^n (a-x) \ln(a-x) + nx I_{n-1,m} + mx I_{n-1,m-1} - m I_{n,m-1}. \tag{14}$$

Thus, the evaluation of $I_{n,m}$ boils down to that of $I_{0,m}$ and $I_{n,0}$. The integral $I_{n,0}$ can be easily obtained by application of (14) n times with $m = 0$.

To evaluate $I_{0,m}$, we first use the following identity:

$$\ln|x-y| = \ln(y-x) = \ln y + \ln\left(1-\frac{x}{y}\right) = \ln y - \sum_{k=1}^{\infty}\frac{1}{k}x^k y^{-k},$$

substitution of the above identity into (9c) with $n=0$ leads to:

$$\int_x^a (\ln y)^m \ln|x-y|\mathrm{d}y = \int_x^a (\ln y)^{m+1}\mathrm{d}y - \sum_{k=1}^{\infty}\frac{1}{k}x^k\int_x^a y^{-k}(\ln y)^m\mathrm{d}y. \quad (15)$$

The integrals on the right hand side of (15) can be computed by using (7a) – (7c), and the special case of (9c) with $n=0$ is proved by noting that the end result consists of the sum of two terms. The first term is x times a $(m+1)$-th order polynomial of $\ln x$; and the second term is a converging power series of x for $0 < x \le a-\epsilon < a$.

Finally, the combination of (9b) and (9c) leads to (9d). □

The following corollary is an immediate consequence of (9d) and will be used in the proof of Theorem 2.

Corollary 1. *Suppose that the functions $K(x)$, $f(x)$, $g(x)$ all admit a power series representation on $[0,a]$. Then*

$$\int_0^a K(x-y)\ln|x-y|f(y)\mathrm{d}y = r(x)\,x\ln x + s(x), \quad (16a)$$

$$\int_0^a K(x-y)f(y)y^n(\ln y)^n\ln|x-y|\mathrm{d}y = x^{n+1}\sum_{k=0}^{n+1}p_k(x)(\ln x)^{n+1-k} + q(x), \quad (16b)$$

where $n > 0$, and the functions $r(x)$, $s(x)$, $p_k(x)$, and $q(x)$ are all smooth and admit a power series representation on $[0, a-\epsilon]$.

Proof. (16a) follows from (9d) by setting $m=0$ and (16b) follows from (9d) directly. □

3 Main Theoretical Results

We rewrite (1a) in the following standard form

$$(\mathsf{I} - \mathsf{K})u = f, \tag{17}$$

where f is defined in Eq. (1b), I is the identify operator, and the operator $\mathsf{K} : L^p(I) \to L^p(I)$, for $1 \le p \le \infty$, is defined as the following:

$$[\mathsf{K}u](x) = \int_I K(x,\, y)u(y)\mathrm{d}y, \quad K(x,\, y) := \frac{1}{k\sqrt{\pi}} J_{-1}\left(\frac{|x-y|}{k}\right), \tag{18}$$

with $I = [-1/2,\, 1/2]$. Note that

$$\|\mathsf{K}\|_p := \left[\int_I |K(x,\, y)|^p \,\mathrm{d}y\right]^{1/p}, \quad \|\mathsf{K}\|_\infty := \max_{x\in I} \int_I |K(x,\, y)|\,\mathrm{d}y. \tag{19}$$

Our main theoretical results concerning the integral equation (1a), or equivalently (17), are summarized in Theorems 1 and 2 and Corollary 2. Theorem 1 proves the existence and uniqueness of the solution. Theorem 2 and Corollary 2 reveals the exact nature of the singularities of the solution at the end points.

Theorem 1. *For any $k > 0$ and $1 \le p \le \infty$,*

1. *K is a compact operator from $L^p(I)$ to $L^p(I)$;*
2. *$\|\mathsf{K}\|_p \le [1 - J_0(1/2k)/J_0(0)] < 1$;*
3. *The integral operator $(\mathsf{I} - \mathsf{K})$ is invertible and its bounded inverse is given by the Neumann series $(\mathsf{I} - \mathsf{K})^{-1} = \sum_{n=0}^{\infty} \mathsf{K}^n$;*
4. *The integral equation $(\mathsf{I} - \mathsf{K})u = f$ has a unique solution for any $f \in L^p(I)$.*

Proof. It is clear from (4) that J_{-1} is only logarithmically singular at $x = y$. So the kernel of K [defined by (18)] is a *continuous kernel of order* 0 and thus K is compact on $L^p(I)$ to $L^p(I)$ for any $0 \le p \le \infty$ (cf. p. 123 in [14]).

We now compute $\|\mathsf{K}\|_\infty$ explicitly as follows;

$$\begin{aligned}
\|\mathsf{K}\|_\infty &= \max_{x\in I}\int_I |K(x,y)|\mathrm{d}y \\
&= \max_{x\in I}\frac{1}{k\sqrt{\pi}}\int_I J_{-1}\left(\frac{|x-y|}{k}\right)\mathrm{d}y \\
&= \max_{x\in I}\frac{1}{k\sqrt{\pi}}\left[\int_{-1/2}^{x} J_{-1}\left(\frac{x-y}{k}\right)\mathrm{d}y + \int_x^{1/2} J_{-1}\left(\frac{y-x}{k}\right)\mathrm{d}y\right] \\
&= \max_{x\in I}\frac{1}{\sqrt{\pi}}\left[J_0\left(\frac{x-y}{k}\right)\Big|_{-1/2}^{x} - J_0\left(\frac{y-x}{k}\right)\Big|_{x}^{1/2}\right] \qquad (20)\\
&= \max_{x\in I}\frac{2}{\sqrt{\pi}}\left\{J_0(0) - \frac{1}{2}\left[J_0\left(\frac{1+2x}{2k}\right) + J_0\left(\frac{1-2x}{2k}\right)\right]\right\} \\
&= \frac{2}{\sqrt{\pi}}\left[J_0(0) - J_0\left(1/2k\right)\right] = 1 - \frac{J_0\left(1/2k\right)}{J_0(0)} \\
&< 1,
\end{aligned}$$

where the equalities are all obvious and the first inequality follows from the convexity of J_0 and the last inequality follows from the monotonicity of J_0 and the property (d) of J_n in Sec. 2.

Since the kernel of the operator is symmetric, $\|\mathsf{K}\|_1 = \|\mathsf{K}\|_\infty$. And the result for general $p \in (1,\,\infty)$ follows from generalized Young's inequality (cf. p. 9 [14]). It then follows naturally that $(\mathsf{I}-\mathsf{K})$ is invertible and its inverse is represented by a converging Neumann series. Hence, by the Fredholm alternative theorem [22], the integral equation (17) has a unique solution for any $f \in L^p(I)$ for $p \in [1,\,\infty]$. □

The next theorem concerns the singularities of the solution of Eq. (1a) at the endpoints. Obviously, the singularities of the solution at both endpoints are identical due to the symmetry of the flow, thus we only need to study the singularity at one endpoint, say, at $y = -1/2$. We first make a simple change of variable to move the interval $[-1/2,\,1/2]$ to $[0,\,1/k]$ so Eq. (1a) becomes

$$u(x) - \frac{1}{\sqrt{\pi}}\int_0^{1/k} J_{-1}\left(|x-y|\right)u(y)\mathrm{d}y = \frac{1}{2\sqrt{\pi}}\left[J_0\left(\frac{1}{k}-x\right) - J_0\left(x\right)\right]. \quad (21)$$

We will still use K to denote the integral operator on the left-hand side and f to denote inhomogeneous term on the right-hand side of Eq. (21).

Theorem 2. *Let*

$$a_0 = \frac{1}{2}\min\left(\frac{1}{k},\, 1\right), \quad a_n = \left(1 - \frac{1}{4n^2}\right) a_{n-1}, \quad F_n(x) := [\mathsf{K}^n f](x), \quad n = 1,\, 2,\, \ldots,$$

then for $k > 0$ and $0 < x < a_n$,

$$F_n(x) = q(x) + \sum_{m=1}^{n+1} p_m(x)(x \ln x)^m, \tag{22}$$

where $q(x)$ and $p_m(x)$ are converging power series in x. That is, for each n, $F_n(x)$ has new singular terms $p_{n+1}(x)(x \ln x)^{n+1}$, of which the new leading singular term is $(x \ln x)^{n+1}$. Hence, the solution u of Eq. (21) *can be represented by the following converging double power series:*

$$u(x) = \sum_{n=0}^{\infty}\sum_{m=0}^{\infty} c_{n,m} x^n (x \ln x)^m, \quad x < a_\infty := \frac{2}{\pi} a_0. \tag{23}$$

Proof. From Theorem 1, the solution u can be written in terms of a converging Neumann series:

$$u(x) = \sum_{n=0}^{\infty} [\mathsf{K}^n f](x) := \sum_{n=0}^{\infty} F_n(x),$$

thus (23) is a simple consequence of (22) and the fact that

$$a_\infty = a_0 \prod_{n=1}^{\infty} \left(1 - \frac{1}{4n^2}\right) = \frac{2}{\pi} a_0.$$

We now show by induction that (22) is true.

The first term in the Neumann series is simply

$$F_0(x) = f(x) = \frac{1}{2\sqrt{\pi}} \left[J_0\left(\frac{1}{k} - x\right) - J_0\left(x\right) \right],$$

and by (4) it is of the form $(x \ln x) h_0(x) + f_0(x) + x g_0(x)$ with h_0, f_0, g_0 all power series of x^2 on $(0,\, a_0)$. So (22) is true for $n = 0$. Assume now that

$F_{n-1}(x)$ is of the form $x^n \sum_{k=0}^{n} p_k(x)(\ln x)^{n-k} + q(x)$ for $0 < x < a_{n-1}$. We will show that $F_n(x)$ is of the form (22) for $0 < x < a_n$.

Since K is a compact operator with logarithmic singularity and f is in $C^\alpha([0,\, 1/k])$ for any $0 < \alpha < 1$, F_n is in $C^\alpha([0,\, 1/k])$.

Clearly,

$$F_n(x) := (\mathsf{K}F_{n-1})(x) := \int_0^{1/k} K(x,\, y)F_{n-1}(y)\mathrm{d}y.$$

We now split the integral into two parts

$$\begin{aligned} F_n(x) =& \int_0^{a_{n-1}} K(x,\, y)F_{n-1}(y)\mathrm{d}y + \int_{a_{n-1}}^{1/k} K(x,\, y)F_{n-1}(y)\mathrm{d}y \\ :=& \Psi_1(x) + \Psi_2(x). \end{aligned} \tag{24}$$

For $0 < x < a_n$, $K(x, y)$ is smooth on the second integration interval $[a_{n-1},\, 1/k]$ in (24) since x is away from the interval. Thus $\Psi_2(x)$ is smooth and can be expressed as a power series on $[0,\, a_n]$.

We now consider $\Psi_1(x)$. Since $K(x,\, y) = \frac{1}{\sqrt{\pi}} J_{-1}(|x-y|)$, by (4) we have

$$K(x,y) = K_1(x-y) + |x-y|K_2(x-y) + \ln|x-y|K_3(x-y),$$

where K_i, $i = 1,\, 2,\, 3$, are all smooth functions. We can split $\Psi_1(x)$ further into three parts

$$\begin{aligned} \Psi_1(x) :=& L_1(x) + L_2(x) + L_3(x) \\ =& \int_0^{a_{n-1}} K_1(x-y)F_{n-1}(y)\mathrm{d}y \\ &+ \int_0^{a_{n-1}} K_2(x-y)|x-y|F_{n-1}(y)\mathrm{d}y \\ &+ \int_0^{a_{n-1}} K_3(x-y)\ln|x-y|F_{n-1}(y)\mathrm{d}y. \end{aligned} \tag{25}$$

It follows from the induction assumption on F_{n-1} and (8) that $L_1(x)$ is smooth on $[0, a_n]$. And by (9a), the most singular term in $L_2(x)$ is $x^{n+2}(\ln x)^n$. Also, by (16a), (16b) and the induction assumption, $L_3(x)$ contains all singular terms in F_{n-1} and the new term $(x \ln x)^{n+1} p_{n+1}(x)$.

Finally, (22) is proved by combining the above results. □

The following Corollary shows that all leading singular terms $(x \ln x)^m$ exist so long as the first leading singular term $(x \ln x)$ appears in the solution.

Corollary 2. *The coefficients $c_m := c_{0,m}$ of the leading singular terms $(x \ln x)^m$ in the solution $u(x)$ given by the double power series of Eq.* (23) *are fully determined by $u(0)$ as follows:*

$$c_m = -\frac{1}{k\sqrt{\pi}m^2} c_{m-1}, \quad c_1 = -\frac{1}{k\sqrt{\pi}} \left[\frac{1}{2} + u(0) \right], \qquad m > 1. \tag{26}$$

Proof. From the properties of J_n given in Section 2, we have

$$J_0(x) = f_0(x) + (x \ln x) h_0(x), \quad h_0(0) = 1. \tag{27}$$

It is obvious that the right hand side function f in (17) has the $x \ln x$ term with the coefficient $-1/(2k\sqrt{\pi})$ and has no higher order singular terms $(x \ln x)^m$ for $m > 1$. From the properties of J_{-1}, it is clear that the most singular term in the kernel $K(x, y)$ is $-(\ln |x - y|)/k\sqrt{\pi}$.

By (9d), it can be shown that the only contribution for $(x \ln x)^m$ by $[\mathsf{K}u](x)$ is due to the term

$$-\frac{1}{k\sqrt{\pi}} \int_0^1 \ln |x-y| c_{m-1} (y \ln y)^{m-1} \mathrm{d}y = -\frac{1}{k\sqrt{\pi}} \frac{1}{m^2} c_{m-1} (x \ln x)^m, \quad m \geq 1. \tag{28}$$

By matching the singular terms $(x \ln x)^m$ on both sides of (17), for $m = 1$, and since $c_0 = u(0)$, we obtain

$$c_1 + \frac{1}{k\sqrt{\pi}} u(0) = -\frac{1}{2k\sqrt{\pi}}. \tag{29}$$

For $m > 1$, we have

$$c_m + \frac{1}{k\sqrt{\pi}} \frac{1}{m^2} c_{m-1} = 0. \tag{30}$$

Rearranging (29) and (30), we obtain (26). □

With the theorems and corollary stated above, the mathematical nature of the integral equation (1a) and its solution are completely understood.

4 Numerical Algorithm

In what follows, we will describe the numerical algorithm to solve Eq. (1a), which is characterized by two key features. First, the kernel $J_{-1}(|x-y|)$ has both logarithmic and absolute value singularities at the diagonal, that is,

$$J_{-1}(|x-y|) = \phi_{-1}(x-y) + g_{-1}(x-y)|x-y| + h_{-1}(x-y)\ln|x-y|,$$

where ϕ_{-1}, g_{-1}, and h_{-1} are smooth functions. And second, both the right-hand side and the solution are singular at the end points $x = \pm 1/2$. To be more precise, if we shift the left endpoint $x = -1/2$ to the origin, then the inhomogeneous term f is of the form $\phi(x) + g(x)x\ln x$ with smooth functions ϕ and g, and the singularities of the solution u are described in detail by (23).

To solve Eq. (1a), we will employ some advanced modern techniques for solving integral equations with singular kernel and corner singularities. Since our problem is one-dimensional, thus it is relatively small in size and the computational speed is not of a concern. To obtain accurate solutions of benchmark quality for the problem, we employ a collocation method in which the collocation points are chosen adaptively with finer and finer mesh toward the end points in order to capture the singularity of the solution at the end points. The underlying integrals are then computed *via* either high order generalized Gaussian quadratures for singular functions (cf. *e.g.*, [28, 41, 6]) or an automatic adaptive Gaussian integrator with the prescribed precision 10^{-30}. We would like to remark here that there have been some recent work on efficient and accurate treatment on corner singularities based on the Nyström method (cf. *e.g.*, [19, 5] and references therein), albeit with a slightly lower accuracy.

In the ensuing discussion, the interval $[-1/2,\, 1/2]$ is transformed to $[0,\, 1] := I$. The interval I is divided into N_m+2 equispaced subintervals, and then each end subinterval is refined dyadically into N_e smaller and smaller subintervals — the closer to an endpoint, the smaller the subinterval. Altogether, the total number of intervals is $N_s = N_m + 2N_e$. For the p-th order method, the solution is approximated by a polynomial of degree $(p-1)$ on each subinterval I_i, and the collocation points on I_i are the Legendre abscissas on I transferred to I_i. Thus, the total number of collocation points N is $p \times N_s$.

The interaction matrix A is constructed as follows. It is clear that A can be decomposed into $N_s \times N_s$ number of $p \times p$ blocks. Denote the ij-th block

of A by $[\mathsf{A}]_{ij}$. Obviously, the k-th row of $[\mathsf{A}]_{ij}$, $\mathbf{r}_k$, is from the discretization of the integral I_j, *i.e.*, the i-th element of $\mathbf{r}_k$ is

$$r_{ki} = \int_{I_j} K(x_{i,k},\, y)u(y)\mathrm{d}y,$$

where $x_{i,k}$ is the k-th collocation point on the subinterval I_i.

For off-diagonal blocks of A, *i.e.*, $[\mathsf{A}]_{ij}$ with $i \neq j$, we first use an adaptive Gaussian integrator with a prescribed precision to compute

$$v_{ki} := \int_{I_j} K(x_{i,k},\, y)p_n(y)\mathrm{d}y,$$

where p_n is the $(n-1)$-th order Legendre polynomial. We then have

$$\mathbf{r}_k = \mathbf{v}_k \cdot \mathsf{P}, \quad \mathbf{v}_k := (v_{k1},\, v_{k2},\, \ldots, v_{kp}),$$

where P is the $p \times p$ Gauss-Legendre transform matrix, of which the elements are the coefficients of a Legendre expansion of a given function on Gauss-Legendre abscissas. Note that P only needs to be computed once *a priori* and stored if necessary. Also, the integrals here are very easy to compute numerically since the collocation points are away from the integration interval and the integrand is thus smooth.

The diagonal blocks of A can be computed similarly, though the involved integrals are harder to compute numerically since the integrand is singular. However, the overall computational cost for computing the diagonal blocks is about the same as that for off-diagonal ones because there are much fewer diagonal blocks than off-diagonal ones. Moreover, we can apply generalized Gaussian quadratures to compute diagonal blocks so that the computational cost is reduced, for the kernel $K(x,\, y)$ is merely weakly singular with two known singularities, *i.e.*, logarithmic and absolute value singularities. The procedure is as follows. For each Legendre abscissa x_k, $k = 1,\, 2,\, \cdots,\, p$, on the standard interval $[0,\, 1]$, we apply generalized Gaussian quadrature algorithm to find a set of quadrature abscissas $\{y_n\}$ and the corresponding weights $\{w_n\}$ such that the function f can be approximated by the quadrature with a prescribed precision:

$$\int_0^1 f(y)\mathrm{d}y = \sum_{n=1}^{n_k} w_n f(y_n), \tag{31a}$$

$$f(y) = \psi_1(y) + \psi_2(y)|x_k - y| + \psi_3(y)\ln|x_k - y|, \tag{31b}$$

where ψ_m, $m = 1, 2, 3$, are polynomials of degree less than, say, $3p$. Then the following integral can also be approximated by the quadrature:

$$\int_{I_j} K(x_{j,k},\, y)u(y)\mathrm{d}y \approx \sum_{n=1}^{n_k} \hat{w}_n K(x_{j,k},\, \hat{y}_n)u(\hat{y}_n), \tag{32}$$

where $\hat{w}_n$ and $\hat{y}_n$ are scaled weights and (shifted) abscissas, respectively, and $u(\hat{y}_n)$ can be obtained *via* Legendre interpolation from $\{x_{j,k}\}$ to $\{\hat{y}_n\}$. The weights and abscissas of the generalized Gaussian quadrature to evaluate the singular integrals in (31) are listed in the appendix section so that our results can be easily reproduced.

5 Numerical Results

This Section presents the evidence to illustrate the performance of the algorithm and provides some benchmark solutions for a wide range of Knudsen number $0.003 \leq k \leq 10.0$. As in Section 4, the interval is shifted to $[0, 1]$ from $[-1/2, 1/2]$.

We implement the algorithm outlined in the preceding section in `Fortran`. We used the `gcc` compiler (version 4.8.1) with the option `--freal-8-real-16` on a 64 bit Linux workstation with a 2.93GHz Intel Xeon CPU which has six cores and 12 MB of cache. The compiling option `--freal-8-real-16` is used so that the quadruple precision is used in the computation. We have also used `OpenMP` to parallelize the computation for constructing the matrix as well as matrix-vector products in `GMRES`. The linear system is then solved using `GMRES` without `OpenMP`. The required precision for `GMRES` is set to 10^{-24}.

With $k = 0.003$, the linear system is rather ill-conditioned and it takes about 430 iterations for `GMRES` to converge to 24 significant digits. We use Linux system command `time` to measure the elapsed time. The elapsed time for the entire calculation is about 62.8 seconds and this is the longest time among the cases studied in this work. With $k = 10.0$, the linear system is well conditioned and it only takes 10 iterations for `GMRES` to converge to 24 significant digits. The elapsed time is only about 23.9 seconds.

5.1 End point singularities

The accuracy of the solution of (1a) critically depends on the resolution of the endpoint singularities. To demonstrate that our algorithm can effectively

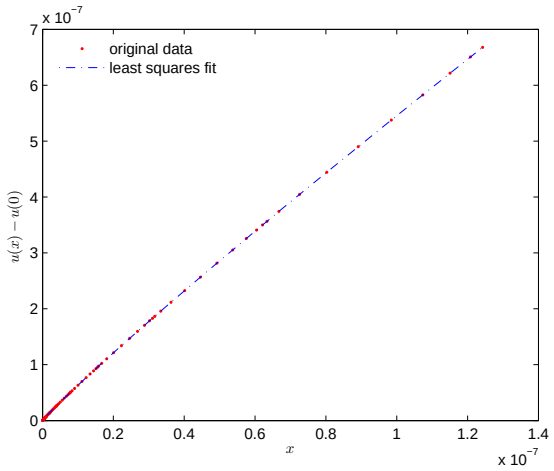

Figure 1: The numerical solution of $u(x) - u(0)$ and its least squares fit on a small interval near the origin. The (red) dots and dashed line represent the numerical solution and the least squares fit $l(x) = -0.6068046x - 0.37601602637x \ln x + 3.409260x^2 \ln x + 1.749711(x \ln x)^2$, respectively.

capture the leading-order singularities $(x \ln x)^m$, $m \geq 1$, near the shifted end point $x = 0$, we compute the solution $u(x)$ in a very small interval $(0,\, a)$, $a \approx 1.5 \cdot 10^{-7}$, and then fit the solution of $u(x) - u(0)$ with the following formula:

$$l(x) = c_{1,0}x + c_1 x \ln x + c_{2,1}x^2 \ln x + c_2(x \ln x)^2. \tag{33}$$

The numerical solution of $u(x,\, k) - u(0,\,)$, $k = 0.03$, is obtained with the number of collocation points $N = 2,000$. Using 240 points of the numerical solution of $u(x) - u(0)$ which are closest to the endpoint $x = 0$, the L^2 or the mean squared error of the least-square fitting with Eq. (33) is $3.4 \cdot 10^{-30}$. The values of the coefficients of $x \ln x$ and $(x \ln x)^2$, *i.e.*, c_1 and c_2 in Eq. (33), computed from (26) are -0.3760160283459086 and 1.767869386997996, respectively, while the values obtained by the least-square fitting are -0.37601602637 and 1.749711, respectively. Clearly, the leading order singular term $x \ln x$ is accurately captured numerically — the numerical value of c_1 agrees with its analytic value for eight significant digits. This accuracy is maintained for all values of the Knudsen number k used in this work.

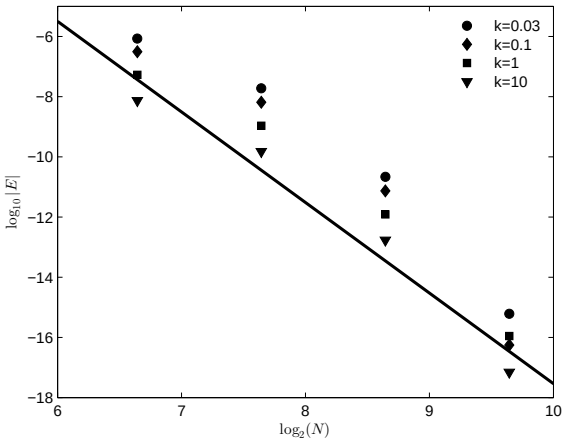

Figure 2: The relative L^2 error of the velocity $u(x)$ versus the total number of discretization point N on log-log scale. The solid line has a slope of $-10\log_{10}(2)$.

5.2 Convergence

To demonstrate the effectiveness of our solution method, we compute the L^2 error for the velocity $u(x)$

$$E := \sqrt{\frac{\int_I \|u_N(x) - u_*(x)\|^2 \mathrm{d}x}{\int_I \|u_*(x)\|^2 \mathrm{d}x}}, \tag{34}$$

where the reference solution $u_*(x)$ is obtained with $N = 2000$ for $k = 0.03$ and $N = 1600$ for other values of k, *i.e.*, $k = 0.1$, 1.0, and 10.0, and the integrals are computed by using the Gauss-Legendre quadrature described in Sec. 4. We use $p = 10$ in our calculations unless otherwise stated.

Figure 2 shows the L^2 error E for the velocity $u(x,\, k)$ with a few values of the Knudsen number k. In all cases shown in Fig. 2, the rate of convergence is about 10, thus the theoretical order of accuracy has been achieved in all calculations.

5.3 Benchmark solutions

To obtain accurate solution for $u(x,\, k)$, we must first accurately compute the right-hand side of Eq. (1a), $f(x,\, k)$, which is singular at the end points.

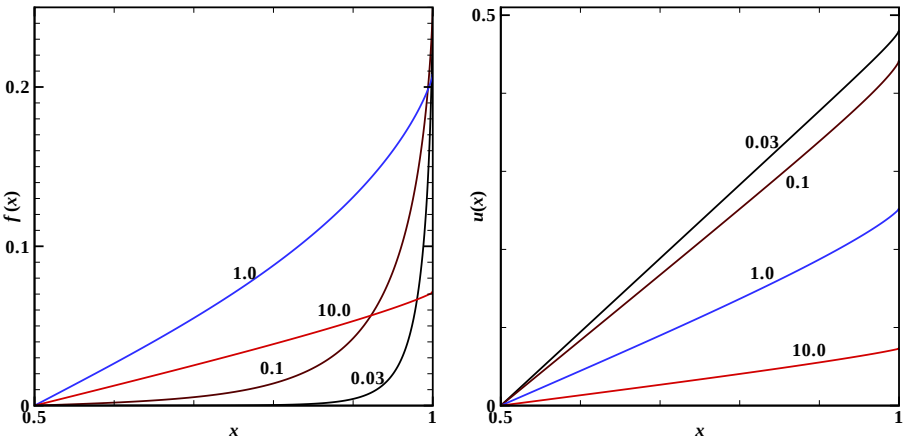

Figure 3: $f(x,\, k)$ (left) and $u(x,\, k)$ (right) for $k = 0.03$, 0.1, 1.0, and 10.0, with the value of k annotated near the corresponding curves.

The properties of $f(x,\, k)$ in fact determine that of the solution $u(x,\, k)$. The Knudsen layers at channel walls are generated by the singularities of $f(x,\, k)$. Figure 3 shows both $f(x,\, k)$ and $u(x,\, k)$ for $k = 0.03$, 0.1, 1.0, and 10.0. Because both $f(x,\, k)$ and $u(x,\, k)$ are anti-symmetric about the channel center $x = 1/2$, Fig. 3 only shows $f(x,\, k)$ and $u(x,\, k)$ in one half of the flow domain $1/2 \le x \le 1$.

It can be shown that near the left end point $x = 0$, the leading-order asymptotic behavior of the inhomogeneous term in the integral equation (1a), f, is

$$f(x,\, k) \sim \frac{1}{2\sqrt{\pi}} \left[\frac{(1-3\gamma)}{2} \frac{1}{k} - \frac{1}{k} \ln \frac{1}{k} + \frac{x}{k} \ln \frac{x}{k} \right], \tag{35}$$

where it is assumed that $1 \gg k \gg x$. Clearly, the leading-order singular term of $f(x,\, k)$ is $(x/k) \ln(x/k)$ for a fixed k. The behavior of f is illustrated in the left panel of Fig. 3.

As shown in Fig. 3, qualitatively, the velocity $u(x,\, k)$ appears to be very close to a straight line, which is the solution of the Navier-Stokes equation, and especially so for very small and large k. Although it is not clearly shown

in the figure, it can be proved that the velocity derivative does not exist at the end points, *i.e.*, the velocity $u(x,\, k)$ is tangent to the channel walls at the boundaries [23].

We now provide the numerical results. In addition to the velocity $u(x,\, k)$, we also provide the velocity derivative at the channel center, $u'(x = \frac{1}{2},\, k)$. It can be shown that $u(x = 1,\, k) \leq 1/2$ and $u'(x = \frac{1}{2},\, k) \geq 1$ for $k \geq 0$. The values of $u(x = 1,\, k)$ and $u'(x = \frac{1}{2},\, k)$ allow us to define the microscopic slip velocity and macroscopic one, respectively. Table 1 provides the data of $u(x,\, k)$ in the upper half channel at $y = 0.6,\, 0.7,\, 0.8,\, 0.9$, and 1.0, and Table 2 provides the data for velocity at the boundary, $u(x = 1,\, k)$ and $u'(x = \frac{1}{2},\, k)$; the values of $u(x = 1,\, k)$ are taken from Table 1 with $N = 1600$. Apparently, the solution of $u(x,\, k)$ converges as the total number of collocation points N increases. It can be seen that the results of $u(x,\, k)$ are accurate for at least twelve significant digits independent of the values of x and k.

we also compute the stress $P_{xy}(k)$ and the half-channel total mass flow rate $Q(k)$:

$$P_{xy}(k) = -\frac{1}{\sqrt{\pi}} \left[\frac{2}{k} \int_{1/2}^{1} J_0\left(x/k\right)\, u(x)\, \mathrm{d}x + J_1\left(1/2k\right) \right], \tag{36}$$

$$Q(k) = \int_{1/2}^{1} u(x,\, k)\, \mathrm{d}x \tag{37}$$

It can be shown that $0 \geq P_{xy}(k) > -1/2\sqrt{\pi}$ and $1/4 \geq Q(k) > 0$ for $k \in [0,\, \infty)$. The results of both $P_{xy}(k)$ and $Q(k)$ are given in Table 3. Since both $P_{xy}(k)$ and $Q(k)$ are integrated from $u(x,\, k)$, their precision should be comparable to that of $u(x,\, k)$ or better.

6 Conclusions

In this paper we have studied in detail the integral equation derived from the linearized BGK equation with the Maxwell diffusive boundary condition for the steady Couette flow. We have proved the existence and uniqueness for the solution of the integral equation. We have shown that the solution of the velocity u near an endpoint can be represented by a converging double power series in terms of $x^m(\ln x)^n$, where x is the distance to the endpoint, and determined semi-analytically the coefficients of the leading order singular terms $(x \ln x)^n$ $(n = 1, 2, 3, \cdots)$.

Table 1: The values of the velocity $u_N(x,\, k)$ at $x = 0.6,\ 0.7,\ 0.8,\ 0.9$, and 1.0, for $0.003 \leq k \leq 10.0$ and $400 \leq N \leq 1600$.

x	0.6	0.7	0.8	0.9	1.0
N			$k = 0.003$		
400	0.09939398007244217	0.1987879601448843	0.2981819402173285	0.3975759203785835	0.4978915175888030
800	0.09939398014204283	0.1987879602840856	0.2981819404261305	0.3975759206569863	0.4978915352788807
1600	0.09939398014207544	0.1987879602841508	0.2981819404262283	0.3975759206571167	0.4978915352789693
			$k = 0.01$		
400	0.09800810020241383	0.1960162013012055	0.2940243425786597	0.3920355719207134	0.4930697754531371
800	0.09800810022280691	0.1960162013419917	0.2940243426398391	0.3920355720023112	0.4930697807741956
1600	0.09800810022280926	0.1960162013419964	0.2940243426398461	0.3920355720023207	0.4930697807742208
			$k = 0.03$		
400	0.09425510233079511	0.1885155964989118	0.2828084717603230	0.3773525608775003	0.4800058665530938
800	0.09425510233708972	0.1885155965115045	0.2828084717792374	0.3773525609029753	0.4800058682766751
1600	0.09425510233708991	0.1885155965115049	0.2828084717792380	0.3773525609029764	0.4800058682766829
			$k = 0.1$		
400	0.08356104029274617	0.1673490502283097	0.2518108070975897	0.3383684060663754	0.4412246405122556
800	0.08356104029425423	0.1673490502313504	0.2518108071022446	0.3383684060729892	0.4412246409722400
1600	0.08356104029425424	0.1673490502313504	0.2518108071022446	0.3383684060729897	0.4412246409722421
			$k = 0.3$		
400	0.06645430069459216	0.1335709509472140	0.2023607233387561	0.2751706693573815	0.3672125694339120
800	0.06645430069493926	0.1335709509479253	0.2023607233398804	0.2751706693590903	0.3672125695500499
1600	0.06645430069493927	0.1335709509479253	0.2023607233398804	0.2751706693590906	0.3672125695500504
			$k = 1.0$		
400	0.04453194115206441	0.08976290005945922	0.1366691806914674	0.1872336429972648	0.2518613399698612
800	0.04453194115212170	0.08976290005957814	0.1366691806916597	0.1872336429975758	0.2518613399894732
1600	0.04453194115212171	0.08976290005957814	0.1366691806916597	0.1872336429975760	0.2518613399894732
			$k = 2.0$		
400	0.03283175101362668	0.06620080866800679	0.1008399340224033	0.1381797101408611	0.1852462993677936
800	0.03283175101364504	0.06620080866804505	0.1008399340224655	0.1381797101409661	0.1852462993740218
1600	0.03283175101364504	0.06620080866804505	0.1008399340224655	0.1381797101409662	0.1852462993740218
			$k = 3.0$		
400	0.02678842250716726	0.05400761302339581	0.08223931900196659	0.1126006454389917	0.1504282444961314
800	0.02678842250717640	0.05400761302341487	0.08223931900199767	0.1126006454390459	0.1504282444992069
1600	0.02678842250717640	0.05400761302341487	0.08223931900199767	0.1126006454390460	0.1504282444992075
			$k = 5.0$		
400	0.02021810350612312	0.04074510549514082	0.06199427039072078	0.08474655782849507	0.1126351880282314
800	0.02021810350612680	0.04074510549514850	0.06199427039073332	0.08474655782851835	0.1126351880294590
1600	0.02021810350612680	0.04074510549514850	0.06199427039073332	0.08474655782851842	0.1126351880294592
			$k = 7.0$		
400	0.01655896140054647	0.03335952222887089	0.05072335823656649	0.06925336240175322	0.09171689613455394
800	0.01655896140054846	0.03335952222887504	0.05072335823657328	0.06925336240176656	0.09171689613521612
1600	0.01655896140054846	0.03335952222887504	0.05072335823657328	0.06925336240176661	0.09171689613521435
			$k = 10.0$		
400	0.01324840054213267	0.02667954575379200	0.04053574032131034	0.05526789346648103	0.07292211299294639
800	0.01324840054213370	0.02667954575379414	0.04053574032131383	0.05526789346648848	0.07292211299328582
1600	0.01324840054213370	0.02667954575379414	0.04053574032131383	0.05526789346648851	0.07292211299328496

Table 2: The dependence of the velocity at boundary $x = 1$, $u(1, k)$, and the velocity derivative at the channel center $x = \frac{1}{2}$, $u'(\frac{1}{2}, k)$, on the Knudsen number k. The results are obtained with an adaptive mesh with $N = 1600$ (with 96 subintervals of equal length in the middle, 32 dyadic refinements towards each end point, and 10 Legendre nodes on each subinterval).

k	$u(1, k)$	$u'(1/2, k)$
0.003	0.4978915352789693	0.9939398014207545
0.01	0.4930697807742208	0.9800810020043015
0.03	0.4800058682766829	0.9425456003244014
0.1	0.4412246409722421	0.8352857656469417
0.3	0.3672125695500504	0.6635300770297120
1.0	0.2518613399894732	0.4442284697467991
2.0	0.1852462993740218	0.3274745769375018
3.0	0.1504282444992075	0.2672070059395808
5.0	0.1126351880294592	0.2016944318181617
7.0	0.09171689613521435	0.1652086347955840
10.0	0.07292211299328496	0.1321955790519311

Table 3: The dependence of the stress P_{xy} and the total mass flow rate Q on the Knudsen number k.

k	P_{xy}	Q
0.003	$-1.490943352367889 \cdot 10^{-3}$	$1.242445655299117 \cdot 10^{-1}$
0.01	$-4.900408001825383 \cdot 10^{-3}$	$1.225330275292619 \cdot 10^{-1}$
0.03	$-1.413798633505404 \cdot 10^{-2}$	$1.180147037188893 \cdot 10^{-1}$
0.1	$-4.155607785109222 \cdot 10^{-2}$	$1.057028408172292 \cdot 10^{-1}$
0.3	$-9.344983511581808 \cdot 10^{-2}$	$8.560111699820618 \cdot 10^{-2}$
1.0	$-1.694625753369582 \cdot 10^{-1}$	$5.804708735555459 \cdot 10^{-2}$
2.0	$-2.083322536749625 \cdot 10^{-1}$	$4.281659776113917 \cdot 10^{-2}$
3.0	$-2.266437497658175 \cdot 10^{-1}$	$3.489298506190833 \cdot 10^{-2}$
5.0	$-2.446632678456018 \cdot 10^{-1}$	$2.627042060967383 \cdot 10^{-2}$
7.0	$-2.536943539674489 \cdot 10^{-1}$	$2.147460412330841 \cdot 10^{-2}$
10.0	$-2.611624603488409 \cdot 10^{-1}$	$1.714449048590649 \cdot 10^{-2}$

We have also developed a high-order numerical algorithm to obtain accurate solution of the integral equation in a wide range of the Knudsen number $0.003 \leq k \leq 10.0$. The results include the flow velocity $u(x, k)$, the stress $P_{xy}(k)$, and the half-channel total mass flow rate $Q(k)$, all of which are accurate for at least twelve significant digits. To the best of our knowledge, our results presented in this work are more accurate than any existing data in literature and can be used as benchmark data. Our algorithm is highly efficient. The order of accuracy is 10; and in the worse case of $k = 0.003$, the elapsed time for the entire calculation is only about a minute on a computer with six cores.

The analysis and the numerical algorithm used here can be easily extended to analyze and solve the integral equations for Kramer's problem and Poiseuille flow. These problems are currently under investigation, and the results will be reported in the future.

Acknowledgements

S. Jiang was supported by the National Science Foundation under grant DMS-1418918 and would like to thank Dr. Zydurnas Gimbutas at NIST for helpful discussions. L.-S. Luo would like to acknowledge the support from the Richard F. Barry Jr. Endowment from Old Dominion University. Part of this work was done in the Summer of 2014 when S. Jiang was visiting Computational Science Research Center in Beijing, China.

Appendix

In this appendix, we list the quadrature nodes and weights for evaluating the integrals of the form $\int_0^1 f(y)dy$ accurately. Here $f(y) = p_1(y)+|x_k-y|p_2(y)+\ln|x_k-y|p_3(y)$, p_m $(m = 1, 2, 3)$ are polynomials of degree less than 30. And x_k $(k = 1, \cdots, 10)$ is the kth Legendre node on the interval $[0, 1]$. These quadrature nodes and weights are used to construct the diagonal blocks of the interaction matrix when discretizing (1a). We list only the nodes and weight for $k = 1, \cdots, 5$ since the nodes and weights for $k = 6, \cdots, 10$ can be obtained by symmetry.

Table 4: Quadrature nodes and weights for evaluating the integrals of the form $\int_0^1 f(y)dy$ to 20 digits accuracy. Here $f(y) = p_1(y) + |x_1 - y|p_2(y) + \ln|x_1 - y|p_3(y)$, p_m $(m = 1, 2, 3)$ are polynomials of degree less than 30. And $x_1 = 0.13046735741414139961017993957774D-01$ is the first Legendre node on the interval $[0, 1]$. The total number of nodes is $N_q = 33$.

Nodes	Weights
0.27361297485236776838079233805786D-03	0.69715918863927482587936388878439D-03
0.13981248979415673972094063568956D-02	0.15249428568017074703142701441109D-02
0.32494632545338047435766917388499D-02	0.21319781765161862242607933626978D-02
0.55571871791008959938149628561218D-02	0.24259030259139066664254567232723D-02
0.79813336339094382034728772776548D-02	0.23620691926887834135310125378059D-02
0.10166831257733026401120075633747D-01	0.19572848772317397067547051323501D-02
0.11812205187544836414708635964200D-01	0.13043891992937108391034075623804D-02
0.12751628804381828377333449225651D-01	0.58239640352911521556335138683259D-03
0.13095540236894367636096767571405D-01	0.31898929480954596681910386363590D-03
0.13921702909769691336670011496194D-01	0.15258572126897478788162344662853D-02
0.16514912312015834902753580283205D-01	0.38524798143095400662335720967952D-02
0.22018347454497919119504046826820D-01	0.73507449337868651374490050211168D-02
0.31600157223664767138258197016357D-01	0.11997134295565287542464781724224D-01
0.46357240301082041297731782375312D-01	0.17674791424247526400543785961529D-01
0.67229240299299707045561986246507D-01	0.24188950315338331200055002367540D-01
0.94929527062693039346454342923203D-01	0.31284875661764443996235675687498D-01
0.12989432147038871636622261452423D+00	0.38665979798699112570347186486431D-01
0.17224962334715982841693225208708D+00	0.46011230378251565243650552946727D-01
0.22179505768086480520244843888682D+00	0.52991553558184285249692056826844D-01
0.27800357156901472651972358969191D+00	0.59285114590127280977241452325236D-01
0.34003579740800511331131417552540D+00	0.64591341486524025486215893449343D-01
0.40676772710109930853192693568386D+00	0.68643481973865389921783244234615D-01
0.47683009634950505289170569430656D+00	0.71219416561776057651226397490653D-01
0.54865758138845680500090923609856D+00	0.72150418352539847316227214158960D-01
0.62054560286841858401834186294081D+00	0.71327560971335279704712574716567D-01
0.69071225666370191755718058487788D+00	0.68705530712522789832178942561527D-01
0.75736269308885698925450134765816D+00	0.64303697472401764260748544768562D-01
0.81875318776462958937644959121359D+00	0.58204440341640794728525627776212D-01
0.87325223008268283477826423618168D+00	0.50548902917711804228526257284161D-01
0.91939623129235971601054281777223D+00	0.41530558652890845720945128211496D-01
0.95593794768874600718691473570761D+00	0.31387204124129287519009750747279D-01
0.98188656742326485860265527240884D+00	0.20392657107551411988760906402873D-01
0.99654260738155551982027436000422D+00	0.88609651267227450497587475835892D-02

Table 5: Quadrature nodes and weights for evaluating the integrals of the form $\int_0^1 f(y)dy$ to 20 digits accuracy. Here $f(y) = p_1(y) + |x_2 - y|p_2(y) + \ln|x_2 - y|p_3(y)$, p_m $(m = 1, 2, 3)$ are polynomials of degree less than 30. And $x_2 = 0.67468316655507744633951655788253D - 01$ is the second Legendre node on the interval $[0, 1]$. The total number of nodes is $N_q = 35$.

Nodes	Weights
0.79298898824604556403037550234537D-03	0.20268884747165843217289939913646D-02
0.41069334637885541516890777539034D-02	0.45572361730293242208709517357174D-02
0.97830619119727169304616943665943D-02	0.67162539067542698107475615797352D-02
0.17352871372288895921938073014863D-01	0.83170474608723978729328950680457D-02
0.26183743107727829491076127818500D-01	0.92196644022669478527300245425818D-02
0.35532616013658448065700003573668D-01	0.93462097526407486061993183531664D-02
0.44617125289112225475443380320427D-01	0.86988301142392596125208639777024D-02
0.52703396060582685542822984289185D-01	0.73741990339635165724598254817861D-02
0.59204247540661094438261115071656D-01	0.55688183080388830998409622532957D-02
0.63775592272740865905940628314878D-01	0.35692600281570354570063779774905D-02
0.66394222457943601294725398520250D-01	0.17247439966378033672780554651747D-02
0.67404020103665465929826975661823D-01	0.46014765461513396056654149796928D-03
0.68107984804755323365590470635973D-01	0.13799548240473080533466942041050D-02
0.70677446112879389641183152264613D-01	0.39809832591687460823014823137415D-02
0.76509214965147623729842906182287D-01	0.78960313940096851885790306392945D-02
0.86874467912703170449537221312445D-01	0.13023130518093976830579829241671D-01
0.10289760205062388325770780592424D+00	0.19174406150060247176324063323933D-01
0.12548054489804007716166964662386D+00	0.26095883802822770648436612381955D-01
0.15524582751949258527837740847159D+00	0.33485723973003262596834950967380D-01
0.19249750595519233198016299581867D+00	0.41011641766437255373660911462808D-01
0.23719903593870653472074789881995D+00	0.48327390964758321061489706344527D-01
0.28896716425475543856382518487597D+00	0.55088311900205820581040470089703D-01
0.34708088127640741803250769077796D+00	0.60965887783008273552721474411009D-01
0.41050436970409069900426562503493D+00	0.65661144408715087414890802537762D-01
0.47792267006256120045050708642296D+00	0.68916635398506236795555444944249D-01
0.54778849683913152492325052364909D+00	0.70526705271961303072997570756722D-01
0.61837832562878605929184999650082D+00	0.70345718153691504345351920569761D-01
0.68785557366071384751635309795977D+00	0.68293974021173330037703416100549D-01
0.75433844772913812935800056123416D+00	0.64361098056487916682682727371446D-01
0.81596986000400953100218015107967D+00	0.58606773306887103397748384970550D-01
0.87098673090271604179803138156568D+00	0.51158785901352000904220206706060D-01
0.91778602243055805108669366775610D+00	0.42208465199477500497685593893348D-01
0.95498500108982086533123854440234D+00	0.32003766294761195801550157761688D-01
0.98147370467879930094154623628724D+00	0.20840907003392496220959732474286D-01
0.99646153240652227749348815163566D+00	0.90673813420467529284564463068975D-02

Table 6: Quadrature nodes and weights for evaluating the integrals of the form $\int_0^1 f(y)dy$ to 20 digits accuracy. Here $f(y) = p_1(y) + |x_3 - y|p_2(y) + \ln|x_3 - y|p_3(y)$, p_m $(m = 1, 2, 3)$ are polynomials of degree less than 30. And $x_3 = 0.160295215850487796882836317442 56D{+}00$ is the third Legendre node on the interval $[0, 1]$. The total number of nodes is $N_q = 38$.

Nodes	Weights
0.13231730360399128698497000771581D-02	0.33860789688687769939144824406619D-02
0.68878176499567126816391884992347D-02	0.76924385080117873079294015894327D-02
0.16560799627165284198744721142085D-01	0.11559415504436159405574561150470D-01
0.29781330478329469664078574951890D-01	0.14751672571403811347470608148965D-01
0.45773845720009724231409178049705D-01	0.17074687042678126890392933115837D-01
0.63592040621333621049642448539195D-01	0.18383879438756757136880614756541D-01
0.82176297069313082377025704860484D-01	0.18599860295711371066045772466729D-01
0.10042687851389844374230631207521D+00	0.17724392560392242779528547603831D-01
0.11729244626893488126313155728369D+00	0.15854499566933134296405739961166D-01
0.13186995164755900241525776875586D+00	0.13190172536688931884899684630304D-01
0.14350648195793432798142617969053D+00	0.10029509544475377223012977948392D-01
0.15188764682357497861681469268504D+00	0.67460842421241245770833682602322D-02
0.15709407660288468824171539118147D+00	0.37483817276547604351988805596726D-02
0.15961063169025306716609097669685D+00	0.14268297264412491835878821949451D-02
0.16038069964117580406232628540498D+00	0.58710871479381695388799624702053D-03
0.16178249945850777794055440493232D+00	0.24981469614729116643265613664515D-02
0.16582957372952545444580959579406D+00	0.58109007863711419564126800481741D-02
0.17380799151538394540711565443076D+00	0.10332478897248029940310040863782D-01
0.18683094857139647508040809065913D+00	0.15861524365511222207444840889214D-01
0.20578240888907360889128075636065D+00	0.22143407528239307555655291370998D-01
0.23127137257830174806059270135453D+00	0.28885333617327760760785198149377D-01
0.26360105976849122770116116850592D+00	0.35770880153317642945154844477948D-01
0.30275216233715399006447248576752D+00	0.42473609564992858762507731368743D-01
0.34837927046602099933052927285750D+00	0.48669799015856989538046597967985D-01
0.39981952470429116940445473386992D+00	0.54050107161322959771154446298758D-01
0.45611221050832325195967617738542D+00	0.58329677860803269382641956198108D-01
0.51602730932477800044950784282566D+00	0.61255747963371334232734974588079D-01
0.57809978351211488852243971088059D+00	0.62611176649547516274237312123403D-01
0.64066442562930131920989850276458D+00	0.62211680965661571111999552198437D-01
0.70188467442584800048835585466818D+00	0.59897634611746372357273259966181D-01
0.75978102541538635726239722901925D+00	0.55554517728413926316608121135458D-01
0.81236730796839806289065958719889D+00	0.49371699135396503002265698390418D-01
0.85834488949346403478033459184340D+00	0.42700901163439562588536998903014D-01
0.89830496674147673180334298910570D+00	0.37489102205293457233842399080171D-01
0.93343467440292221758912996089377D+00	0.32582427753392563238989265210426D-01
0.96283106467036394707824682224262D+00	0.25854584730852273003416876563281D-01
0.98452267006137379542492500597257D+00	0.17280666617327564522899713021095D-01
0.99702683807753278615611694390842D+00	0.76089836137228341500421865420411D-02

Table 7: Quadrature nodes and weights for evaluating the integrals of the form $\int_0^1 f(y)dy$ to 20 digits accuracy. Here $f(y) = p_1(y) + |x_4 - y|p_2(y) + \ln|x_4 - y|p_3(y)$, p_m $(m = 1, 2, 3)$ are polynomials of degree less than 30. And $x_4 = 0.28330230293537640460036702841711D + 00$ is the fourth Legendre node on the interval $[0, 1]$. The total number of nodes is $N_q = 40$.

Nodes	Weights
0.17346046123086179780907002321737D-02	0.44420388857473339012473271290236D-02
0.90563864579127074345670357772614D-02	0.10152135182268441462596025564318D-01
0.21892929735140067220305650381109D-01	0.15427129212659299441166464247499D-01
0.39684901549178195207159499240791D-01	0.20025889943207090136916263835980D-01
0.61650062272030896404949601606799D-01	0.23741954364718227422111603633013D-01
0.86817763636662496554666021446463D-01	0.26406447605095700974939063037626D-01
0.11407121327829116783240119535770D+00	0.27897617524894494223154633544460D-01
0.14219966021263811575816901008677D+00	0.28151032976949053513828420705082D-01
0.16996094484419903699987943857273D+00	0.27170042420119922418365010617515D-01
0.19615431025460006502544344733507D+00	0.25035588503565871864668387522890D-01
0.21970179453253080906216745469346D+00	0.21912999255946916534646534343685D-01
0.23973320645583772561130490884202D+00	0.18051563644485388706851402931008D-01
0.25566556487492562901944710724502D+00	0.13774188876861333572041207159972D-01
0.26727515144139551167411497357106D+00	0.94846325041961748935893925836884D-02
0.27484496098160334508271158884352D+00	0.58428241325056204734642935955065D-02
0.27943707450196761317998326096736D+00	0.35483238258440518641527221958544D-02
0.28212751240019090493687439869841D+00	0.18501851175047820194418962465602D-02
0.28323046563761461924435298887377D+00	0.50867662097425498095904824815040D-03
0.28398528881216337792042262637469D+00	0.14579496466221548869801245390629D-02
0.28665295073761903791295418754434D+00	0.40819901478158654893690540881756D-02
0.29253705773734628618336446913235D+00	0.78666095884179944988649919186940D-02
0.30271348676191456868581182058325D+00	0.12631484981365937535319891132552D-01
0.31804941410477038834547993662152D+00	0.18143359191900265986355260540683D-01
0.33915999428820099204591680345723D+00	0.24133895966619859647638376579018D-01
0.36638032047073645920383543216724D+00	0.30313491912262447023524005502289D-01
0.39975055937960329205830359108093D+00	0.36383947660995248867832591889339D-01
0.43901340788402305736661350835388D+00	0.42050476790475910067268742957818D-01
0.48362326621105645523504312269660D+00	0.47033119525369089749324977974917D-01
0.53276647136720393227133272125015D+00	0.51077412826743932765002962078874D-01
0.58539172270149002648636856474130D+00	0.53964055621676270481757555688984D-01
0.64024954344603403216541338303367D+00	0.55517263745602723960818577244105D-01
0.69593931540222693334637846387348D+00	0.55611513436798679683796731797866D-01
0.75096213963090153933592508528961D+00	0.54176410639692367350592568916099D-01
0.80377754264909150957475568686408D+00	0.51199485340487093653956473721450D-01
0.85286188461700732730832405895418D+00	0.46726787735119716132738645240565D-01
0.89676624595435314249702042628151D+00	0.40861250748342762325755906211537D-01
0.93417158103452545327970114430247D+00	0.33758881144671967800293176092201D-01
0.96393905166056910666112301881022D+00	0.25622979687235247613364918941361D-01
0.98515383862338646704502599184142D+00	0.16697128540075353698645768015538D-01
0.99716390102059424905641686459890D+00	0.72672345241651523766589999216984D-02

Table 8: Quadrature nodes and weights for evaluating the integrals of the form $\int_0^1 f(y)dy$ to 20 digits accuracy. Here $f(y) = p_1(y) + |x_5 - y|p_2(y) + \ln|x_5 - y|p_3(y)$, p_m $(m = 1, 2, 3)$ are polynomials of degree less than 30. And $x_5 = 0.42556283050918439455758699943514D+00$ is the fifth Legendre node on the interval $[0, 1]$. The total number of nodes is $N_q = 40$.

Nodes	Weights
0.22088129895183631945412687611112D-02	0.56579825923091213651955355171321D-02
0.11545985774009799126173164199769D-01	0.12962323210589356664281843031007D-01
0.27972165541061541958591692985927D-01	0.19786170071375500355337629626980D-01
0.50868360797368948473916655383052D-01	0.25861226032319771351722973049064D-01
0.79368181277021247759237930672339D-01	0.30958293133935646605960119528082D-01
0.11239526622651432458786361776462D+00	0.34887907209203944975699176391075D-01
0.14870694159418093649817722982154D+00	0.37508191998676875878066853038105D-01
0.18694552953937001605723889109612D+00	0.38732164161574115906252243216946D-01
0.22569655971862686898107273844937D+00	0.38534251228500903202127773225816D-01
0.26355317108360342862766907871124D+00	0.36956177091235267928630665305358D-01
0.29918608150657275060856393673468D+00	0.34112158933655772892977788215140D-01
0.33141812038071410365856876451860D+00	0.30192604621142389351302073108818D-01
0.35930087668961820484084345105543D+00	0.25464153872003234961625292936293D-01
0.38218809591262153421198573088323D+00	0.20262447104782263123751628141482D-01
0.39979654076648402277238490333392D+00	0.14973744601583597819957064951333D-01
0.41224212373475876688267182742174D+00	0.10003989433954399423177478566277D-01
0.42004012476614550838198086193858D+00	0.57390004778579578077050512408776D-02
0.42406464121241732642815501735369D+00	0.25044850577126572209938086537009D-02
0.42547620212284396730342792112400D+00	0.59518816499920221584104471681566D-03
0.42625763999458805149826961208124D+00	0.14441516613813801757710586407276D-02
0.42878546789261738391344958182729D+00	0.37418729122513214832294202848159D-02
0.43395672560094514509754055244173D+00	0.66995156756583187024537842090157D-02
0.44242031127614498255345086848322D+00	0.10376411673315772297518128154903D-01
0.45504803160294997849549917875145D+00	0.15047081808399015303256876655901D-01
0.47278804714584050802910628571125D+00	0.20528158278443939547043397128815D-01
0.49620712870378687514537427696907D+00	0.26320554976669468526066428515932D-01
0.52537927275250196249635360151786D+00	0.31966432134515625976313063974729D-01
0.55996834614609872531849099597983D+00	0.37099527152231463769160248968288D-01
0.59930713645787314271159760850525D+00	0.41420932330168829259051831827720D-01
0.64245850160491103020414911800997D+00	0.44689073508480086293536750635436D-01
0.68827172693503518222784052727189D+00	0.46718438018124237687665045965758D-01
0.73543889826004101736388928991027D+00	0.47380281996657359709529479379849D-01
0.78255204620908121746366714761248D+00	0.46603312422289793030244612045398D-01
0.82816068920501548192093850064065D+00	0.44373729943029350170155832912216D-01
0.87082893114694636174551488355601D+00	0.40734233359980282931705123310400D-01
0.90919090112328625138382989359318D+00	0.35781651421500079267917316660338D-01
0.94200304226427356779313069091916D+00	0.29662986599202944812455481969885D-01
0.96819162871628547888254065766180D+00	0.22569845855657572596529852780374D-01
0.98689406547622102692300045372875D+00	0.14731781918610545374512495829261D-01
0.99749523122399556669785767258235D+00	0.64175673560206340352777337619267D-02

References

[1] M. Abramowitz and I. A. Stegun, *Handbook of Mathematical Functions with Formulas, Graphs, and Mathematical Tables*, National Bureau of Standards, Washington, DC, 1972.

[2] S. Albertoni, C. Cercignani, and L. Gotusso, *Numerical evaluation of the slip coefficient*, Phys. Fluids, 6 (1963), pp. 993–996.

[3] L. B. Barichello, M. Camargo, P. Rodrigues, and C. E. Siewert, *Unified solutions to classical flow problems based on the BGK model*, Z. Angew. Math. Phys., **52** (2001), pp. 517–534.

[4] P. L. Bhatnagar, E. P. Gross, and M. Krook, *A model for collision processes in gases. I. Small amplitude processes in charged and neutral one-component systems*, Phys. Rev., **94** (1954), pp. 511–525.

[5] J. Bremer, *A fast direct solver for the integral equations of scattering theory on planar curves with corners*, J. Comput. Phys., **231** (2012), pp. 1879–1899.

[6] J. Bremer, Z. Gimbutas, and V. Rokhlin, *A nonlinear optimization procedure for generalized Gaussian quadratures*, SIAM J. Sci. Comput., **32** (2010), pp. 1761–1788.

[7] C. Cercignani, *The Boltzmann Equation and Its Applications*, Springer, New York, 1988.

[8] C. Cercignani, *Rarefied Gas Dynamics: From Basic Concepts to Actual Calculations*, Cambridge University Press, Cambridge, UK, 2000.

[9] C. Cercignani, R. Illner, and M. Pulvirenti, *The Mathematical Theory of Dilute Gases*, Springer, New York, 1994.

[10] C. Cercignani, M. Lampis, and S. Lorenzani, *Plane Poiseuille-Couette problem in micro-electro-mechanical systems applications with gas-rarefaction effects*, Phys. Fluids, **18** (2006), p. 087102.

[11] C. Cercignani and C. D. Pagani, *Variational approach to boundary-value problems in kinetic theory*, Phys. Fluids, **9** (1966), pp. 1167–1173.

[12] C. Cercignani and F. Sernagiotto, *Cylindrical Couette flow of a rarefied gas*, Phys. Fluids, **10** (1967), pp. 1200–1204.

[13] F. Coron, *Derivation of slip boundary-conditions for the Navier-Stokes system from the Boltzmann equation*, J. Stat. Phys., **54** (1989), pp. 829–857.

[14] G. B. Folland, *Introduction to Partial Differential Equations*, Princeton University Press, Princeton, 2 ed., 1995.

[15] L. Gibelli, *Velocity slip coefficients based on the hard-sphere Boltzmann equation*, Phys. Fluids, **24** (2012), p. 022001.

[16] I. S. Gradshteyn and I. M. Ryzbik, *Table of Integrals, Series, and Products*, Academic Press, New York, 6th ed., 2000.

[17] E. P. Gross and E. A. Jackson, *Kinetic models and the linearized Boltzmann equation*, Phys. Fluids, **2** (1959), pp. 432–441.

[18] E. P. Gross, E. A. Jackson, and S. Ziering, *Boundary value problems in kinetic theory of gases*, Ann. Phys., **1** (1957), pp. 141–167.

[19] J. Helsing, *Solving integral equations on piecewise smooth boundaries using the RCIP method: A tutorial*, Abstr. Appl. Anal., (2013), p. 938167.

[20] I. N. Ivchenko, S. K. Loyalka, and R. V. Tompson, Jr., *Analytical Methods for Problems of Molecular Transport*, vol. 83 of Fluid Mechanics and its Applications, Springer, Dordrecht, The Netherlands, 2007.

[21] M. N. Kogan, *Rarefied Gas Dynamics*, Plenum Press, New York, 1969.

[22] R. Kress, *Linear Integral Equations*, vol. 82 of Applied Mathematics Sciences, Springer, New York, 3nd ed., 2014.

[23] W. Li, L.-S. Luo, and J. Shen, *Accurate solution and approximations of the linearized BGK equation for steady Couette flow*, Comput. Fluids, **111** (2015), pp. 18–32.

[24] S. K. Loyalka, *Velocity profile in Knudsen layer for Kramer's problem*, Phys. Fluids, **18** (1975), pp. 1666–1669.

[25] S. K. Loyalka, *Some exact numerical results for the BGK model: Couette, Poiseuille and thermal creep flow between parallel plates*, Z. Angew. Math. Phys., **30** (1979), pp. 514–521.

[26] S. K. Loyalka and K. A. Hickey, *The Kramer's problem: Velocity slip and defect for a hard sphere gas with arbitrary accommodation*, Z. Angew. Math. Phys., **41** (1990), pp. 245–253.

[27] S. K. Loyalka and R. V. Tompson, *The velocity slip problem: Accurate solutions of the BGK model integral equation*, Euro. J. Mech. B/Fluids, **28** (2009), pp. 211–213.

[28] J. Ma, V. Rokhlin, and S. Wandzura, *Generalized Gaussian quadrature rules for systems of arbitrary functions*, SIAM J. Numer. Anal., **33** (1996), pp. 971–996.

[29] A. J. MacLeod, *Chebyshev expansions for Abramowitz functions*, Appl. Numer. Math., **10** (1992), pp. 129–137.

[30] F. Sharipov, *Data on the velocity slip and temperature jump on a gas-solid interface*, J. Phys. Chem. Ref. Data, **40** (2011), p. 023101.

[31] F. Sharipov and V. Seleznev, *Data on internal rarefied gas flows*, J. Phys. Chem. Ref. Data, **27** (1998), pp. 657–706.

[32] Y. Sone, *Kinetic theory analysis of the linearized Rayleigh problem*, Phys. Fluids, **7** (1964), pp. 470–471.

[33] Y. Sone, *Molecular Gas Dynamics: Theory, Techniques, and Applications*, Birkhäuser, Boston, 2007.

[34] Y. Sone, S. Takata, and T. Ohwada, *Numerical analysis of the plane Couette flow of a rarefied gas on the basis of the linearized Boltzmann equation for hard-sphere molecules*, Euro. J. Mech. B/Fluids, **9** (1990), pp. 273–288.

[35] M. M. R. Williams, *A review of the rarefied gas dynamics theory associated with some classical problems in flow and heat transfer*, Z. Angew. Math. Phys., **52** (2001), pp. 500–516.

[36] D. R. Willis, *Comparison of kinetic theory analyses of linearized Couette flow*, Phys. Fluids, **5** (1962), pp. 127–135.

[37] L. Wu, J. M. Reese, and Y. Zhang, *Solving the Boltzmann equation deterministically by the fast spectral method: Application to gas microflows*, J. Fluid Mech., **746** (2014), pp. 53–84.

[38] L. Wu, C. White, T. J. Scanlon, J. M. Reese, and Y. Zhang, *Deterministic numerical solutions of the Boltzmann equation using the fast spectral method*, J. Comput. Phys., **250** (2013), pp. 27–52.

[39] Y. W. Yap, *Rarefied Gas Dynamics: Stokes' Second Problem*, honours thesis, The University of Melbourne, Victoria, Australia, 2009.

[40] Y. W. Yap and J. E. Sader, *High accuracy numerical solutions of the Boltzmann Bhatnagar-Gross-Krook equation for steady and oscillatory Couette flows*, Phys. Fluids, **24** (2012), p. 032004.

[41] N. Yarvin and V. Rokhlin, *Generalized Gaussian quadratures and singular value decompositions of integral operators*, SIAM J. Sci. Comput., **20** (1998), pp. 699–718.